Published by
NIGERIAN SOCIETY OF PHYSICAL SCIENCES
Available online @ https://journal.nsps.org.ng/index.php/jnsps

J. Nig. Soc. Phys. Sci. 5 (2023) 1371

Journal of the Nigerian Society of Physical Sciences

Corrosion Inhibition Properties of Lawsone Derivatives againts Mild Steel: A Theoretical Study

Saprizal Hadisaputra*, Lalu Rudyat Telly Savalas

Chemistry Education Division, FKIP, University of Mataram. Jalan Majapahit 62, Mataram, 83125, Indonesia

Abstract

Theoretical studies have been carried out using DFT, *ab initio* MP2 and Monte Carlo (MC) simulations of corrosion inhibitors from lawsone derivatives against carbon steel. The research focuses on studying the effect of substituent groups in the lawsone structure on the efficiency of corrosion inhibition in mild steel. Quantum chemical parameters of lawstone inhibitors in neutral and protonated conditions have been calculated. Fukui's function analysis predicts that the active side of the inhibitor will be adsorbed on the mild steel surface. MC simulation is used to understand the adsorption patterns of lawsone compounds on metal surfaces. The organic inhibitor L-NH_2 has better performance as a corrosion inhibitor for mild steel in neutral or protonated conditions.

DOI:10.46481/jnsps.2023.1371

Keywords: Lawsone, Substituents, DFT, MP2, Monte Carlo, Corrosion inhibitors

Article History :
Received: 26 January 2023
Received in revised form: 21 February 2023
Accepted for publication: 30 March 2023
Published: 14 June 2023

Communicated by: K. Sakthipandi

1. Introduction

Metals are damaged by corrosion as a result of corrosive environmental interactions [1, 2]. Corrosion causes significant economic losses, and harms the environment [3, 4]. The corrosion inhibitors that are currently in use are inorganic and unfriendly to the environment. Therefore, organic inhibitors based on eco-friendly natural ingredients prevent potential corrosion. Plant extracts have reportedly been used as corrosion inhibitors that are safe for the environment [4]. The majority of natural materials are highly effective inhibitors. It is because natural product molecules like alkaloids and flavaloids, which are sources of π-electrons, also include heteroatoms N, O, and S [4]. The natural chemicals that have adsorbed on the surface of the metal and shield it from corrosion attack are responsible for the high value of corrosion inhibition efficiency. El-Etre et al. investigated lawsone as corrosion inhibitors on metals in various environments, including as acids, in experimental study that was previously published. The figure for inhibitory efficiency that was highest was 95.78% for carbon steel, followed by 93.44% for Zn in a NaCl media and 88.77% for Ni in an HCl medium [5,6]. In a different investigation, Dananjaya et al. evaluated the lawstone as a corrosion inhibitor on mild steel in an acidic media and discovered that it was 93.14% effective [5]. Theoretical investigations have shown that substituents in the inhibitor structure can raise the value of inhibitory efficiency.

The mechanism of corrosion inhibition has frequently been explained by theoretical investigations [7]. The challenges that

*Corresponding author tel. no:
Email address: rizal@unram.ac.id (Saprizal Hadisaputra)

experimental research have identified have been successfully addressed by theoretical studies [8]. Molecular structure can be determined using quantum chemistry techniques, which can also be used to explain reactivity and electronic structure. The experimental studies that have already been conducted can be supplemented by quantum chemical computations [9]. The current investigation focuses on the electrical characteristics of the quantum parameters of the lawone derivative. It is thought that substituents alter how far electrons shift inside the inhibitor, which in turn affects how well corrosion is inhibited.

2. Methodology

2.1. Quantum Chemical Parameters

To understand experimental results and explore reaction pathways, quantum chemical simulations have been used extensively [10]. The structural significance of corrosion inhibitors and adsorption on metal surfaces has been satisfactorily described using DFT [11–12,13]. Gaussian 09 [14] implements for density functional theory (DFT) and ab initio MP2 6-311++G (d,p) for quantum chemical calculations in the gas and solution phases. The reactivity of a molecule can be described by quantum chemical characteristics. Charge population and condensed Fukui function are two more variables that can be used to determine local selectivity [16]. Koopmans' theorem states that the values of EHOMO and ELUMO are related to ionization potential I =− EHOMO and electron affinity A=− ELUMO, respectively. The ability of an atom or collection of atoms to draw electrons toward itself is known as electronegativity $\chi=\frac{I+A}{2}$. Atomic resistance to charge transfer is measured by hardness (η) [18, 19]. The hardness value can be used to calculate by $\eta=\frac{I-A}{2}$. The quantity of electrons exchanged: $\Delta N=\frac{\chi \mathrm{Fe}-\chi \mathrm{Inh}}{2(\eta \mathrm{Fe}+\eta \mathrm{Inh})}$, where χFe and χinh represent, respectively, the absolute electronegativities of iron and organic inhibitors. The absolute hardness of iron and organic inhibitors, respectively, are denoted by the symbols ηFe and ηinh. The number of electrons transported is determined using the theoretical values of Fe = 7.0 eV and Fe = 0 [20, 21]. The Fukui function can be used to calculate by f+= q(N + 1) q (N) and f- = q(N) – q(N-1) where the charge an atom has upon accepting electrons is denoted by q(N+1). The charge on an atom in a neutral molecular state is defined by the formula q(N). The charge left on an atom after it loses electrons is known as q(N-1) [22, 23].

2.2. MC simulation Calculations

Material Studio 7.0 was used to do MC simulations [24–25]. The interaction of lawsone derivatives with 100 water molecules on the surface of mild steel was simulated using MC techniques to find the configuration with the lowest adsorption energy [26]. The Fe (110) field can be used to depict the surface of mild steel. Because it is the most stable and has a medium atomic density, the Fe(110) field is employed [27]. A 20 vacuum layer on the C axis and an 8x8 supercell were included in the simulation box (19.859002 x 19.859002 x 34.187956) used to simulate the Fe(110) field [28]. The water dissolving action was simulated by adding 100 geometrically optimized water molecules, each of the organic inhibitors (L-H, L-NH2, L-OCH3, and L-NO2), and the Fe(110) surface to a simulated box using the KOMPASS force field [25]. To simulate the actual corrosion environment, a MC simulation was performed.

3. Results and Discussion

The lawone was evaluated as a corrosion inhibitor on mild steel in hydrochloric acid environment in earlier studies by Dananjaya et al. The weight loss strategy utilized produced a 93.14% inhibitory efficiency score [5]. Henna plant extract, an aromatic hydroxyl chemical, is the source of lawsone. The metal surface will be able to create a more stable structure thanks to the lawsone phenol group's ability to transfer electrons to it. This can inhibit redox reactions and guard against corrosion attacks on metals [29]. In addition, both donor and electron withdrawing groups have the potential to affect the value of inhibition efficiency. First, technique validation was done in this theoretical study. To ensure the accuracy of the technique and the set of bases employed, method validation is done. This is done so that results from theoretical and experimental investigations can be compared. Figure 1 depicts the lawsone's geometric structure. It can be contrasted with the findings of theoretical research and an experimental X-ray study that Salunke-Gawali et al. [30] previously reported. Table 1 shows that there is a 0.0504-unit difference in the Bond distance. The basis sets are suitable for application since the results of the variations in the lawsone's binding distances are fairly modest.

The surfaces of mild steel (Fe) can adsorb lawsone compounds and substituents (NH_2, OCH_3, and NO_2) under neutral or protonated circumstances [31]. Electron transfer is investigated by demonstrating the characteristics of molecular orbitals [15]. EHOMO is typically correlated with an organic inhibitor's ability to provide metals with electrons [32]. Table 3 demonstrates that the organic inhibitor L-NH2 has a larger EHOMO value and a tendency to be able to donate electrons to Fe metal, as measured by -8.6774 eV. The values for electron transport are L-NH2, L-OCH3, L-H, and L-NO2, in that order. As opposed to organic inhibitors L-H, L-OCH3, and L-NO2, L-NH2 is expected to have a higher level of inhibitory efficiency.

In addition to accepting electrons from metal d-orbitals, which results in the creation of back bonds, the value of inhibitory efficiency can also be acquired by donating electrons to the empty d-orbitals of metal ions [33]. As a result, accepting electrons from the empty d-orbitals of metals is made easier by a lower ELUMO value. Table 3 shows L-NH2 had the greatest ELUMO at 0.1850 eV and L-NO2 had the lowest at -0.4789 eV. These findings suggest that the organic inhibitors of L-NO2 are more likely to receive electrons from the Fe d orbital, predicting a decline in efficiency.

The reactivity of atoms and molecules can be characterized by their ionization potential [15]. Due to the atoms' low ionization potential, they are able to donate electrons from organic inhibitors to the metal surface by simply releasing their outer electrons. The high ionization potential value indicates that electrons do not easily escape from the outer shell, which means that there is difficulty in the process of transferring electrons

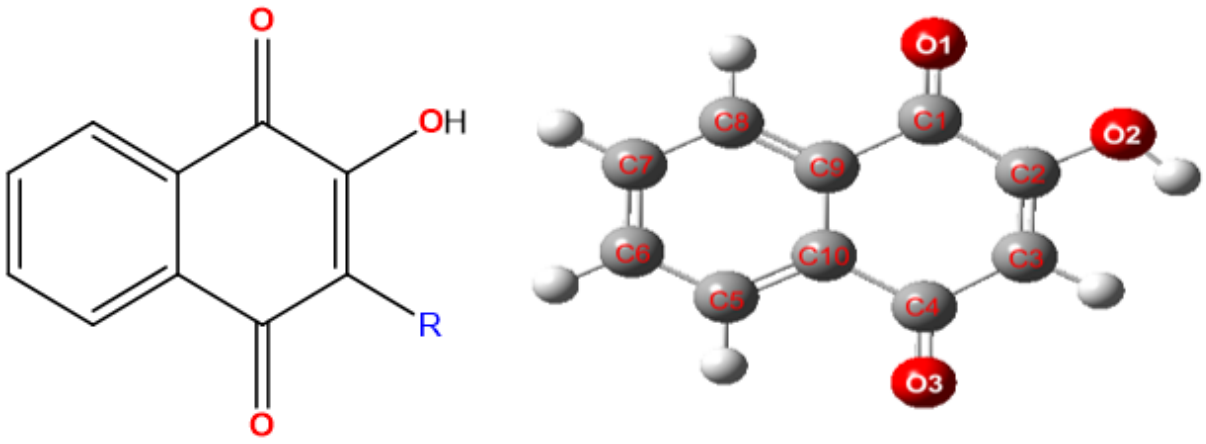

Figure 1: Structure of lawsone (R= -NH_2, OCH_3, NO_2)

Table 1: Comparison of the crystal structure of the lawone compound in the experimental study [30] and the theoretical study of DFT/6-311++G (d,p)

Bond (Å)	Exp [30]	Theory	Bond (Å)	Exp [30]	Theory
C1-O1	1.220	1.22029	C5-C6	1.394	1.39450
C2-O2	1.264	1.34507	C5-H5	0.950	1.08516
C4-O3	1.259	1.22792	C6-C7	1.390	1.39891
C1-C9	1.483	1.48758	C6-H6	0.950	1.08654
C1-C2	1.530	1.50585	C7-C8	1.389	1.39335
C2-C3	1.388	1.35348	C7-H7	0.950	1.08638
C3-C4	1.407	1.46702	C8-C9	1.393	1.39914
C3-H3	0.950	1.08799	C8- H8	0.950	1.08522
C4-C10	1.491	1.49688	C9-C10	1.397	1.40743
C5-C10	1.392	1.39639	-	-	-

Table 2: Quantum chemical characteristics (in eV) of organic inhibitors in gaseous media estimated by DFT and MP2 using a 6-311++G(d,p) level of theory

Inhibitors	EHOMO	ELUMO	ΔE	*I*	*A*	χ	η	ΔN
L-H								
DFT/B3LYP	-7.5272	-3.4436	-4.0836	7.5272	3.4436	5.4854	2.0418	0.3709
Ab initio MP2	-9.8483	0.1905	-10.0388	9.8483	-0.1905	4.8289	5.0194	0.2163
L-NH_2								
DFT/B3LYP	-6.2537	-3.2066	-3.0471	6.2537	3.2066	4.7302	1.5236	0.7449
Ab initio MP2	-8.7414	0.3086	-9.0500	8.7414	-0.3086	4.2164	4.5250	0.3076
PP-OCH_3								
DFT/B3LYP	-6.6268	-3.3718	-3.2550	6.6268	3.3718	4.9993	1.6275	0.6147
Ab initio MP2	-9.2486	0.1502	-9.3988	9.2486	-0.1502	4.5492	4.6994	0.2608
PP-NO_2								
DFT/B3LYP	-7.8570	-4.1963	-3.6607	7.8570	4.1963	6.0266	1.8304	0.2659
Ab initio MP2	-10.3033	-0.6196	-9.6837	10.3033	0.6196	5.4615	4.8419	0.1589

from organic inhibitors to the Fe surface [34]. Table 3 shows the low ionization potential value on L-NH2 is 8.6774 eV while the highest ionization potential value is on L-NO_2 of 9.9471 eV. The organic inhibitor L-NH_2 is more reactive to metal Fe so that it can cause a strong interaction between organic inhibitors and metal Fe. It can be predicted that the organic inhibitor L-NH2 can increase the value of inhibition efficiency. Pan et al. have reported that the experimental ionization potential value for 1,4-naphthaquinone using IR LD/VUV PIMS was found to be 9.52 eV [35]. The results obtained were almost close to the ionization potential value of the organic inhibitor L-H (lawsone) of 9.7926 eV using the ab initio method in aqueous media. Therefore, the ab intio MP2 at 6-311++G (d,p) method is valid to use.

Table 3: The quantum chemical characteristics (in eV) of organic inhibitors in aqueous environments determined using DFT and MP2 with a 6-311++G(d,p) level of theory

Inhibitors	EHOMO	ELUMO	ΔE	*I*	*A*	χ	η	ΔN
L-H								
DFT/B3LYP	-7.4219	-3.5035	-3.9184	7.4219	3.5035	5.4627	1.9592	0.3923
Ab initio MP2	-9.7926	0.1162	-9.9088	9.7926	-0.1162	4.8382	4.9544	0.2182
L-NH_2								
DFT/B3LYP	-6.1835	-3.3157	-2.8678	6.1835	3.3157	4.7496	1.4339	0.7847
Ab initio MP2	-8.6774	0.1850	-8.8625	8.6774	-0.1850	4.2462	4.4312	0.3107
L-OCH_3								
DFT/B3LYP	-6.6273	-3.4733	-3.1541	6.6273	3.4733	5.0503	1.5770	0.6182
Ab initio MP2	-9.2483	0.0465	-9.2949	9.2483	-0.0465	4.6009	4.6474	0.2581
L-NO_2								
DFT/B3LYP	-7.8475	-4.0904	-3.7571	7.8475	4.0904	5.9690	1.8785	0.2744
Ab initio MP2	-9.9471	-0.4789	-9.4682	9.9471	0.4789	5.2130	4.7341	0.1887

Table 4: The quantum chemical characteristics (in eV) of protonated organic inhibitors determined using DFT and MP2 in a 6-311++G(d,p) in gaseous media

Inhibitors	EHOMO	ELUMO	ΔE	*I*	*A*	χ	η	ΔN
Pronated L-H								
DFT/B3LYP	-11.6394	-8.2804	-3.3590	11.6394	8.2804	9.9599	1.6795	-0.8812
Ab initio MP2	-13.6748	-4.7081	-8.9667	13.6748	4.7081	9.1915	4.4834	-0.2444
Pronated L-NH_2								
DFT/B3LYP	-10.7471	-8.1474	-2.5998	10.7471	8.1474	9.4473	1.2999	-0.9413
Ab initio MP2	-13.1058	-4.7557	-8.3501	13.1058	4.7557	8.9308	4.1750	-0.2312
Pronated L-OCH_3								
DFT/B3LYP	-10.9319	-8.2570	-2.6749	10.9319	8.2570	9.5945	1.3374	-0.9699
Ab initio MP2	-13.4060	-4.8469	-8.5591	13.4060	4.8469	9.1264	4.2795	-0.2484
Pronated L-NO_2								
DFT/B3LYP	-12.0519	-8.7101	-3.3418	12.0519	8.7101	10.3810	1.6709	-1.0117
Ab initio MP2	-14.0941	-5.1383	-8.9558	14.0941	5.1383	9.6162	4.4779	-0.2921

Table 5: Quantum chemical characteristics (in eV) of protonated organic inhibitors in aqueous media as computed using DFT and MP2 in a 6-311++G(d,p) level of theory

Inhibitors	EHOMO	ELUMO	ΔE	*I*	*A*	χ	η	ΔN
Pronated L-H								
DFT/B3LYP	-8.1177	-4.6654	-3.4523	8.1177	4.6654	6.3915	1.7262	0.1762
Ab initio MP2	-10.2720	-1.0814	-9.1907	10.2720	1.0814	5.6767	4.5953	0.1440
Pronated L-NH_2								
DFT/B3LYP	-7.0450	-4.6338	-2.4112	7.0450	4.6338	5.8394	1.2056	0.4813
Ab initio MP2	-9.4592	-1.2120	-8.2472	9.4592	1.2120	5.3356	4.1236	0.2018
Pronated L-OCH_3								
DFT/B3LYP	-7.4235	-4.7650	-2.6586	7.4235	4.7650	6.0943	1.3293	0.3407
Ab initio MP2	-9.9305	-1.3124	-8.6181	9.9305	1.3124	5.6215	4.3091	0.1600
Pronated L-NO_2								
DFT/B3LYP	-8.4192	-5.0341	-3.3851	8.4192	5.0341	6.7267	1.6925	0.0807
Ab initio MP2	-10.4484	-1.4066	-9.0418	10.4484	1.4066	5.9275	4.5209	0.1186

Theoretical values of Fe = 7 eV and Fe = 0 eV can be used to calculate the amount of electron transfer from organic inhibitors to Fe metal surfaces. The inhibition efficiency value obtained from the electron donation of organic inhibitors to Fe metal coincides with the electron transfer value [37]. Organic inhibitors' ability to give electrons can do so to mild steel's surface (Fe 110). According to Table 2-5, the values for electron transfer are as follows: L-NH2 > L-OCH3 > L-H > L-NO2. Table 3 shows that the greatest electron transfer value in L-NH2 was measured at 0.3107 eV using the MP2/6-311++G

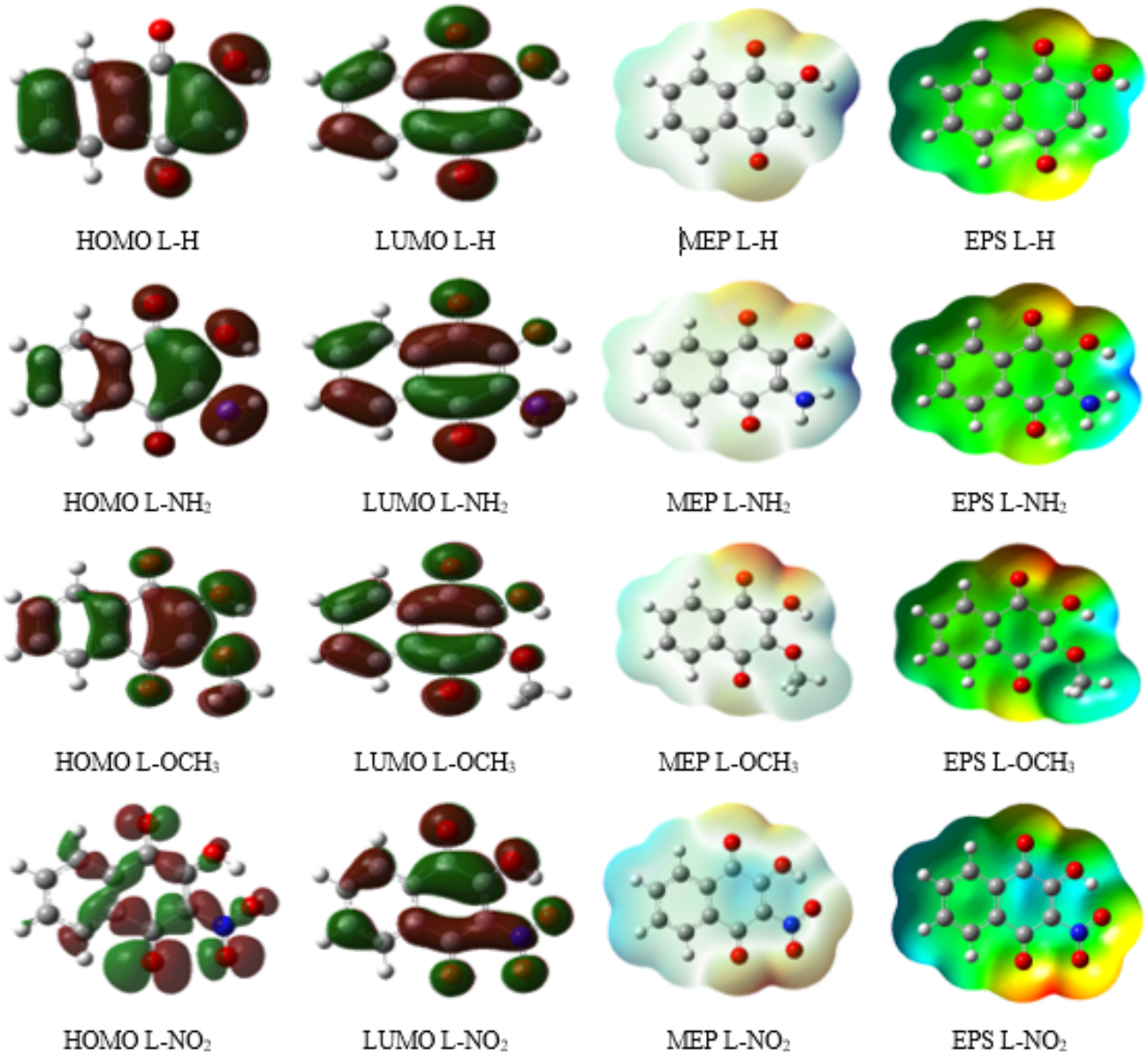

Figure 2: HOMO, LUMO orbitals, MEP and ESP of the studied molecules

(d,p) technique. These findings provide credence to the idea that organic inhibitors can bind to metal surfaces during electron donor-acceptor interactions. L-NH2 is therefore expected to be the best corrosion inhibitor.

The HOMO, LUMO, ESP, and MEP molecular orbital coefficients can represent the region around a molecule, and the electron probability density can provide information about the size and electrophilicity of the molecule [38]. Figure 2 illustrates the visualization of HOMO, LUMO, ESP, and MEP using the DFT/6-311++G (d,p) approach to describe the mechanism of adsorption on metal surfaces. In order to identify the reactive side of a molecule, ESP visualization offers a visual way for comprehending regions that have higher electron density than other regions. In ESP, the color red denotes the highest negative electrostatic potential, blue denotes the most positive electrostatic potential, and green denotes zero electrostatic potential [15]. Red, orange, yellow, green, and blue are in ascending order of electrical potential [31]. On the oxygen atom of the lawstone carbonyl in the organic inhibitor L-NH2, there is a yellow hue. It is possible that oxygen atoms will get up on the surface of the metal Fe (110) by adsorptive means. However, the Fukui function is a more accurate way to assess the electron density of the area of the molecule that is exposed to electrophilic or nucleophilic attack [39].

Fukui function was proposed by Parr and Yang 1984 [40] as a measure of local reactivity indicating the presence of reactive site regions in molecules such as nucleophilic and electrophilic attack [41]. The preferred site for nucleophilic attack is the atom in a molecule that has the maximum functional value (f+) due to its association with ELUMO.

Table 6: Fukui Functional analysis of L-H, L-NH2, L-OCH3, PP-NO2 molecules

L-H	N-	N	N+	f+	f-
C1	-0.3892	-0.3764	-0.3521	0.0242	0.0129
C2	-0.3095	-0.2896	-0.2386	0.051	0.0199
C3	0.1960	0.2655	0.3007	0.0415	0.0695
C4	0.2357	0.1893	0.2046	0.0153	-0.0464
C5	0.3801	0.3155	0.3413	0.0258	-0.0645
C6	0.1601	0.2399	0.2834	0.0435	0.0798
C7	-0.7657	-0.6214	-0.5695	0.0518	**0.1443**
C8	0.3974	0.4442	0.5449	**0.1007**	0.0467
C9	0.0173	0.0293	0.0270	-0.0023	0.0119
C10	-0.8073	-0.7433	-0.7462	-0.0030	0.0641
O11	-0.3682	-0.2058	-0.1222	0.0836	**0.1624**
O12	-0.3918	-0.2495	-0.1551	**0.0944**	**0.1422**
O13	-0.2239	-0.1801	-0.0594	**0.1207**	0.0437
$L\text{-}NH_2$	N-	N	N+	f+	f-
C1	-0.3939	-0.3661	-0.3428	0.0232	0.0278
C2	-0.3352	-0.3209	-0.3015	0.0194	0.0144
C3	0.1255	0.2094	0.2422	0.0329	0.0839
C4	0.1674	0.1023	0.1057	0.0033	-0.0651
C5	0.7316	0.7209	0.7438	0.0229	-0.0107
C6	0.2215	0.2871	0.3259	0.0388	0.0656
C7	-1.0085	-0.8464	-0.8297	0.0167	**0.1621**
C8	0.6826	0.6309	0.6519	0.0210	-0.0517
C9	-0.0923	-0.0581	0.0037	0.0618	0.0342
C10	-0.7777	-0.7120	-0.7230	-0.0110	0.0657
O11	-0.3733	-0.2305	-0.1309	**0.0996**	**0.1428**
O12	-0.4217	-0.2731	-0.2040	0.0692	**0.1486**
O13	-0.2321	-0.1923	-0.0572	**0.1351**	0.0398
N14	-0.5461	-0.4994	-0.3365	**0.1629**	0.0467
$L\text{-}OCH_3$	N-	N	N+	f+	f-
C1	-0.3773	-0.3638	-0.3401	0.0237	0.0135
C2	-0.4298	-0.4051	-0.3838	0.0213	0.0247
C3	0.1725	0.2412	0.2745	0.0334	0.0687
C4	0.3175	0.2375	0.2323	-0.0052	-0.0800
C5	0.5314	0.4988	0.4992	0.0004	-0.0327
C6	0.1279	0.1853	0.2101	0.0247	0.0574
C7	-0.2970	-0.1380	-0.0629	0.0751	**0.1590**
C8	0.1008	0.1620	0.2823	**0.1202**	0.0612
C9	-0.1741	-0.1835	-0.1872	-0.0037	-0.0093
C10	-0.5862	-0.5174	-0.5504	-0.0330	0.0688
O11	-0.3681	-0.2174	-0.1288	0.0886	**0.1507**
O12	-0.3942	-0.2484	-0.1674	0.0810	**0.1458**
O13	-0.2453	-0.1946	-0.0523	**0.1423**	0.0507
O14	-0.3666	-0.3370	-0.2289	**0.1081**	0.0296
C15	-0.2889	-0.2944	-0.3132	-0.0188	-0.0056
$L\text{-}NO_2$	N-	N	N+	f+	f-
C1	0.3589	-0.3603	-0.3591	0.0012	-0.7192
C2	-0.3791	-0.3404	-0.2778	0.0626	0.0386
C3	0.3035	0.3356	0.3809	0.0453	0.0321
C4	0.3187	0.2703	0.2703	0.0000	-0.0484
C5	0.4743	0.4862	0.5675	0.0814	0.0118
C6	0.1983	0.2693	0.3215	0.0521	0.0711
C7	-0.6848	-0.6217	-0.5946	0.0271	0.0631
C8	0.8653	0.8424	0.8908	0.0484	-0.0229

C9	-0.3609	-0.2941	-0.2849	0.0092	0.0667
C10	-0.9140	-0.8509	-0.8439	0.0070	0.0631
O11	-0.3236	-0.1723	-0.0865	**0.0858**	**0.1513**
O12	-0.2651	-0.1732	-0.0992	0.0740	**0.0919**
O13	-0.2064	-0.1374	-0.0504	**0.0870**	0.0690
N14	-0.5459	-0.5019	-0.4841	0.0178	0.0440
O15	0.0364	0.1259	0.2000	**0.0741**	**0.0895**
O16	-0.0538	0.0282	0.0892	0.0611	0.0819

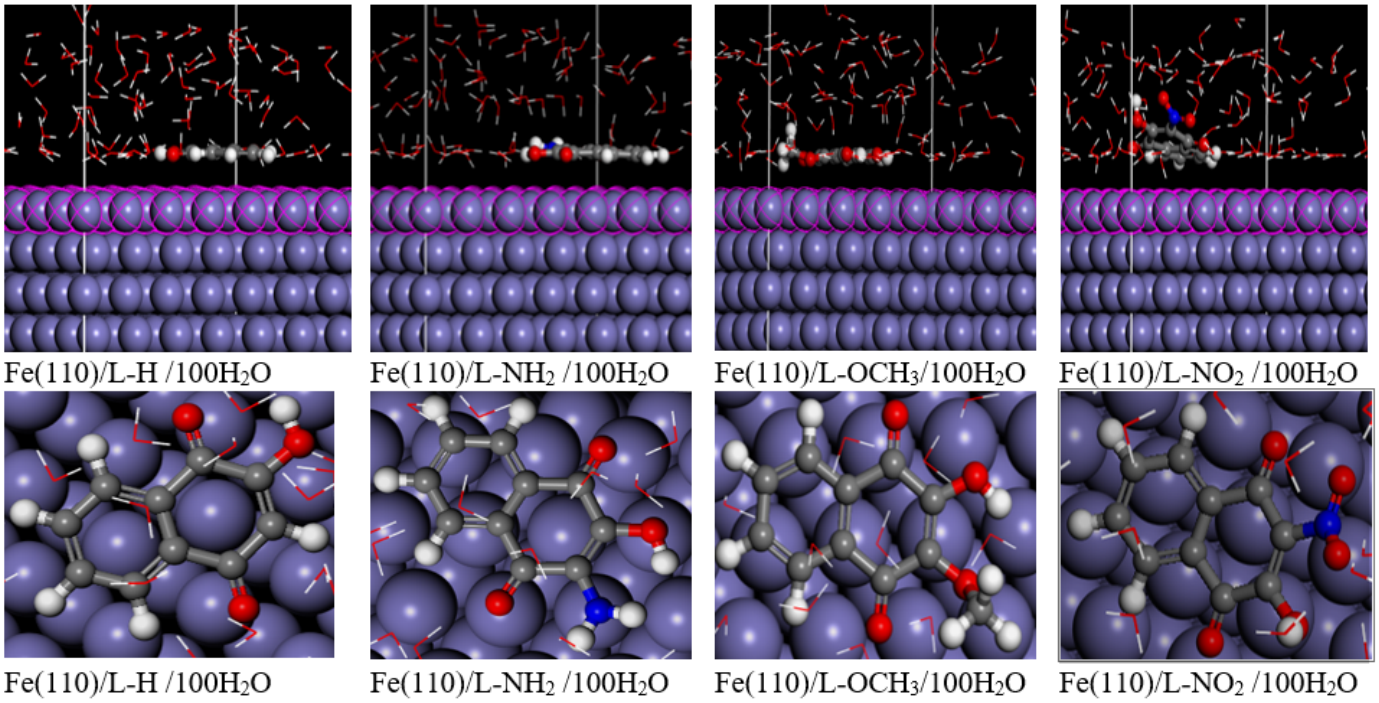

Figure 3: Adsorption of organic inhibitors (L-H, L-NH_2, L-OCH_3, L-NO_2) on ferrous metal surfaces in the MC Fe(110)/inhibitor/100H_2O system

Table 7: Adsorption energy of organic inhibitors (L-H, L-NH_2, L-OCH_3, L-NO_2) Fe(110)/inhibitor/100H2O system using MC simulation

Systems	Adsorption energy of inhibitors kcal.mol^{-1}	Adsorption energy of water kcal.mol^{-1}
Neutral Inhibitor		
Fe(110)/L-H /100H_2O	-129.5897925	-13.84984664
Fe(110)/L-NH_2 /100H_2O	-143.4672645	-14.48869095
Fe(110)/L-OCH_3 /100H_2O	-142.3615059	-13.74108729
Fe(110)/ L-NO_2 /100H_2O	-113.8560443	-12.27065388
Protonated Inhibitor		
Fe(110)/L-H /100H_2O	-134.9297789	-13.26018364
Fe(110)/L-NH_2 /100H_2O	-140.5591996	-12.53631498
Fe(110)/L-OCH_3 /100H_2O	-139.2186163	-12.76122573
Fe(110)/ L-NO_2 /100H2O	-88.50163792	-12.41283883

The preferred area for electrophilic attack is the atom in the molecule that has the maximum value of the Fukui function (f-) because it is associated with EHOMO [42]. The value of f- indicates the ability of an atom to donate electrons to the empty d orbitals of metal Fe (110) [8]. Table 7 using the DFT/6-311++G (d,p) method shows that the maximum f+ value of organic inhibitors L-H on atoms (C8, O12, O13), L-NH2 on atoms (O11, O13, N14), L- OCH3 on atoms (C8, O13, O14), L-NO2 on atoms (O11, O13, O15). The atom acts as an electron acceptor because of the back-donation from the Fe metal surface [8]. The maximum f- values of organic inhibitors L-H, L-NH2 and L-OCH3 are found on atoms (C7, O11, O12), L-NO2 on atoms (O11, O12, N14), respectively. Each organic inhibitor on the O11 and O12 atoms tends to donate electrons to the Fe (110) surface so as to form coordinate bonds [43-44].

The most effective way for characterizing the interaction between substrate and adsorbate is the MC simulation approach. The lowest desired adsorption energy arrangement for the adsorbate component on the Fe(110) surface can be found using MC simulation [45]. Figure 3 shows the most stable adsorption energy configuration of each lawsone derivatives under the conditions of 100 water molecules and the Fe (110) surface. Understanding the nature of the adsorption process can be aided by measuring the distance between the atoms in organic inhibitors and the surfaces of Fe metal. The van der Waals force is regarded as being the primary interaction in chemical adsorption (chemissorption) if the value of this distance is less than 3.5. These results prove that the organic inhibitor L-NH_2 has a distance between oxygen atoms in O1 of 3.256 Å, O2 of 3.132 Å and O3 of 3.379 Å and to the surface of Fe (110). The carbonyl (C=O) and hydroxyl (O-H) atoms can donate electrons to the Fe (110) surface to form complex compounds. Since more oxygen atoms contribute as electron donors to the Fe (110) metal surface, the visualization findings of the ESP and Fukui functions confirm this conclusion. In a MC simulation, the lowest energy system across all systems is sought after [46]. The adsorption energy is linked to the energy generated while the relaxed adsorbate is adsorbed on the substrate [47, 48]. Table 7 shows that the highest negative adsorption value for the organic inhibitor L-NH_2 is -142.3615 kcal/mol. This is caused by the interaction between the mesomeric effect and the NH_2 substituent, which serves as an electron donor and facilitates the transfer of electrons to the vacant Fe (110) orbital. In order to create stable coordination bonds, L-NH_2 possesses a lone pair of electrons on the oxygen and nitrogen atoms. In order to create the most stable adsorption layer and shield mild steel from corrosion attack, L-NH2 is therefore more likely to be adsorbed on the surface of Fe (110) [49, 50].

4. Conclusion

The effect of substituents (NH_2, OCH_3, NO_2) to the lawsone structure was studied as a corrosion inhibitor in mild steel using quantum chemical calculations and MC simulations. It is possible to predict quantum chemical characteristics from the structure of corrosion inhibitors. A contribution of electrons to the surface of mild steel metal can be demonstrated by the large value of EHOMO and electron transfer from quantum chemical parameters, allowing for the prediction of an increase in inhibitory efficiency. In comparison to L-H, L-OCH_3, and L-NO_2 in a neutral or protonated state, L-NH_2 can be projected to be the best inhibitor based on all the tests that have been performed.

References

[1] B. E. Rani & B. B. Basu, "Green inhibitors for corrosion protection of metals and alloys: An overview", International Journal of Corrosion (2012) 1.

[2] S. A. Umoren, M. M. Solomon, I. B. Obot & R. K. Suleiman, "A critical review on the recent studies on plant biomaterials as corrosion inhibitors for industrial metals", Journal of Industrial and Engineering Chemistry **76** (2019) 91.

[3] K. Adama & I. Onyeachu, "The corrosion characteristics of SS316L stainless steel in a typical acid cleaning solution and its inhibition by 1-benzylimidazole: Weight Loss, electrochemical and sem characterizations", Journal of the Nigerian Society of Physical Sciences 4 (2022) 214.

[4] T. O. Martins, E. A. Ofudje, A. A. Ogundiran, O. A. Ikeoluwa, O. A. Oluwatobi, E. F. Sodiya & O. Ojo, "Cathodic corrosion inhibition of steel by Musa paradisiaca leave extract", Journal of the Nigerian Society of Physical Sciences **4** (2022) 740.

[5] S. Dananjaya, M. Edussuriya & A. Dissanayake, "Inhibition action of lawsone on the corrosion of mild steel in acidic media", TOJSAT **2** (2016) 32.

[6] A. Y. El-Etre, M. Abdallah & Z. E. El-Tantawy, "Corrosion inhibition of some metals using lawsonia extract", Corrosion Science **47** (2005) 385.

[7] H. Ju, L. Ding, C. Sun & J.-jing Chen, "Quantum chemical study on the corrosion inhibition of some oxadiazoles", Advances in Materials Science and Engineering (2015) 1.

[8] S. Hadisaputra, A. A. Purwoko, Y. Wirayani, M. Ulfa & S. Hamdiani, "Density functional and perturbation calculation on the corrosion inhibition performance of benzylnicotine and its derivatives", In AIP Conference Proceedings, AIP Publishing LLC **224** (2019) 020006.

[9] G. Gece, "The use of quantum chemical methods in corrosion inhibitor studies", Corrosion Science **50** (2008) 2981.

[10] B. T. Ogunyemi & F. K. Ojo, "Corrosion inhibition potential of thiosemicarbazide derivatives on aluminium: Insight from Molecular Modelling and QSARS approaches", Journal of the Nigerian Society of Physical Sciences **5** (2023) 915.

[11] H. R. Obayes, G. H. Alwan, A. H. Alobaidy, A. A. Al-Amiery, A. A. Kadhum & A. B. Mohamad, "Quantum chemical assessment of benzimidazole derivatives as corrosion inhibitors", Chemistry Central Journal **8** (2014) 1.

[12] A. Thomas, T. S. Khan & P. Gupta, "Density functional theory based indicators to predict the corrosion inhibition potentials of ceramic oxides in harsh corrosive media", Physical Chemistry Chemical Physics **25** (2023) 2537.

[13] S. Hadisaputra, A. A. Purwoko, L. R. T. Savalas, N. Prasetyo, E. Yuanita & S. Hamdiani, "Quantum Chemical and Monte Carlo Simulation Studies on Inhibition Performance of Caffeine and Its Derivatives against Corrosion of Copper", Coatings **10** (2020) 1086.

[14] M. J. Frisch, G.W. Trucks, H. B. Schlegel et al., *Gaussian 09*, Gaussian, Inc, Wallingford, CT, (2009).

[15] W. Shu-Yu, H. Wen-Zhi, L. Chang, L. Guang-Ming & Z. Fei-Er, "Characterizations and preparation of Mg(OH)2 nanocrystals through ultrasonic–hydrothermal route", Research on Chemical Intermediates **42** (2015) 4135.

[16] M. Ouakki et al., "Quantum chemical and experimental evaluation of the inhibitory action of two imidazole derivatives on mild steel corrosion in sulphuric acid medium," Heliyon **5** (2019) e02759.

[17] T. Koopmans, "Über die Zuordnung von Wellenfunktionen und Eigenwerten zu den Einzelnen Elektronen Eines Atoms", Physica **1** (1934) 104.

[18] R. G. Parr, L. v. Szentpály & S. Liu, "Electrophilicity Index", Journal of the American Chemical Society **121** (1999) 1922.

[19] W. Yang & R. G. Parr, "Hardness, softness, and the fukui function in the

electronic theory of metals and catalysis", Proceedings of the National Academy of Sciences **82** (1985) 6723.

[20] I. Lukovits, E. Kálmán & F. Zucchi, "Corrosion Inhibitors—Correlation between Electronic Structure and Efficiency", Corrosion **57** (2001) 3.

[21] S. Hadisaputra, A. A., Purwoko, R. Rahmawati, D. Asnawati, I. Ilhamsyah & S. Hamdiani, N. Nuryono, "Experimental and theoretical studies of (2R)-5-hydroxy-7- methoxy-2-phenyl-2,3-dihydrochromen-4-one as corrosion inhibitor for iron in hydrochloric acid", International Journal of Electrochemical Science (2019) 11110.

[22] W. Yang & W. J. Mortier, "The use of global and local molecular parameters for the analysis of the gas-phase basicity of amines," Journal of the American Chemical Society **108** (1986) 5708.

[23] O. Oyeneyin, D. Akerele, N. Ojo & O. Oderinlo, "Corrosion Inhibitive Potentials of some 2H-1-benzopyran-2-one Derivatives- DFT Calculations", Biointerface Research in Applied Chemistry **11** (2021) 13968.

[24] R. L. C. Akkermans, N. A. Spenley & S. H. Robertson, "Monte Carlo methods in Materials Studio", Molecular Simulation **39** (2013) 1153.

[25] V. V. Mehmeti & A. R. Berisha, "Corrosion Study of Mild Steel in Aqueous Sulfuric Acid Solution Using 4-Methyl-4H-1,2,4-Triazole-3-Thiol and 2-Mercaptonicotinic Acid—An Experimental and Theoretical Study", Frontiers in Chemistry **5** (2017).

[26] A. Berisha, "Experimental, Monte Carlo and Molecular Dynamic Study on Corrosion Inhibition of Mild Steel by Pyridine Derivatives in Aqueous Perchloric Acid", Electrochem **1** (2020) 188.

[27] S. Kirkpatrick, C. D. Gelatt & M. P. Vecchi, "Optimization by Simulated Annealing", Science **220** (1983) 4598.

[28] V. Thaçi, R. Hoti, A. Berisha & J. Bogdanov, "Corrosion study of copper in aqueous sulfuric acid solution in the presence of (2E,5E)-2,5-dibenzylidenecyclopentanone and (2E,5E)-bis[(4-dimethylamino)benzylidene]cyclopentanone: Experimental and theoretical study", Open Chemistry **18** (2020) 1412..

[29] W. B. W. Nik, F. Zulkifli, O. Sulaiman, K. B. Samo & R. Rosliza, "Study of Henna (Lawsonia inermis) as Natural Corrosion Inhibitor for Aluminum Alloy in Seawater", IOP Conference Series: Materials Science and Engineering **36** (2012) 012043.

[30] S. Salunke-Gawali, L. Kathawate, Y. Shinde, V. G. Puranik & T. Weyhermüller, "Single crystal X-ray structure of Lawsone anion: Evidence for coordination of alkali metal ions and formation of naphthosemiquinone radical in basic media", Journal of Molecular Structure **1010** (2012) 38.

[31] R. Wati, S. Hadisaputra, D. Asnawati & D. Hermanto, "Protection of copper corrosion in acidic medium using pinostrobin", Acta Chimica Asiana **1** (2018) 50.

[32] I. B. Obot, D. D. Macdonald & Z. M. Gasem, "Density functional theory (DFT) as a powerful tool for designing new organic corrosion inhibitors. Part 1: An overview", Corrosion Science **99** (2015) 1.

[33] E. A. M. Gad, E. M. S. Azzam & S. A. Halim, "Theoretical approach for the performance of 4-mercapto-1-alkylpyridin-1-ium bromide as corrosion inhibitors using DFT", Egyptian Journal of Petroleum **27** (2018) 695.

[34] S. Hadisaputra, A. A. Purwoko & S. Hamdiani, "Substituents effects on the corrosion inhibition performance of pyrazolone against Carbon Steels: Quantum Chemical and Monte Carlo Simulation Studies", International Journal of Corrosion and Scale Inhibition **10** (2021) 419.

[35] Y. Pan et al., "Intramolecular hydrogen transfer in the ionization process of α-alanine", Physical Chemistry Chemical Physics **11** (2009) 1189.

[36] M. Yadav, D. Behera & S. Kumar, "Experimental and theoretical investigation on adsorption and corrosion inhibition properties of imidazopyridine derivatives on mild steel in hydrochloric acid solution", Surface and Interface Analysis **46** (2014) 640.

[37] S. M. Hosseini, M. J. Bahrami & P. Pilvar, "Adsorption effect of 1-((2-hydroxynaphtalen-1-YL) (phenyl)methyl)urea on the carbon steel corrosion in hydrochloric acid media," Materials and Corrosion **61** (2009) 866.

[38] M. A. Bedair, "The effect of structure parameters on the corrosion inhibition effect of some heterocyclic nitrogen organic compounds", Journal of Molecular Liquids **219** (2016) 128.

[39] B. Idir & F. Kellou-Kerkouche, "Experimental and theoretical studies on corrosion inhibition performance of phenanthroline for cast iron in acid solution," Journal of Electrochemical Science and Technology **9** (2018) 260.

[40] R. G. Parr & W. Yang, "Density functional approach to the frontier-electron theory of chemical reactivity", Journal of the American Chemical Society **106** (1984) 4049.

[41] T. W. Quadri, L. O. Olasunkanmi, O. E. Fayemi, H. Lgaz, O. Dagdag, E.-S. M. Sherif, A. A. Alrashdi, E. D. Akpan, H.-S. Lee & E. E. Ebenso, "Computational insights into quinoxaline-based corrosion inhibitors of steel in HCL: Quantum Chemical Analysis and QSPR-Ann Studies", Arabian Journal of Chemistry **15** (2022) 103870.

[42] S. Kumar, D. G. Ladha, P. C. Jha & N. K. Shah, "Theoretical study of chloro-N-(4-methoxybenzylidene)aniline derivatives as corrosion inhibitors for zinc in hydrochloric acid", International Journal of Corrosion (2013) 1.

[43] Z. El Adnani, M. Mcharfi, M. Sfaira, M. Benzakour, A. T. Benjelloun & M. Ebn Touhami, "DFT theoretical study of 7-r-3methylquinoxalin-2(1h)-thiones (RH; CH3; cl) as corrosion inhibitors in hydrochloric acid", Corrosion Science **68** (2013) 223.

[44] S. Hadisaputra, Z. Iskandar & D. Asnawati, "Prediction of the corrosion inhibition efficiency of imidazole derivatives: A Quantum Chemical Study", Acta Chimica Asiana **2** (2019) 88.

[45] M. Rbaa, A. S. Abousalem, M. Galai, H. Lgaz, B. Lakhrissi, I. Warad & A. Zarrouk, "New N-heterocyclic compounds based on 8-hydroxyquinoline as efficient corrosion inhibition for mild steel in HCL Solution: Experimental and theoretical assessments", Arabian Journal for Science and Engineering **46** (2020) 257.

[46] S. John, R. Jeevana, K. K. Aravindakshan, and A. Joseph, "Corrosion inhibition of mild steel by N(4)-substituted thiosemicarbazone in hydrochloric acid media", Egyptian Journal of Petroleum **26** (2017) 405.

[47] S. Hadisaputra, S. Hamdiani, M. A. Kurniawan, and N. Nuryono, "Influence of macrocyclic ring size on the corrosion inhibition efficiency of Dibenzo crown ether: A Density Functional Study", Indonesian Journal of Chemistry **17** (2017) 431.

[48] S. Hadisaputra, A. A. Purwoko & S. Hamdiani, "Copper Corrosion Protection by 4-Hydrocoumarin Derivatives: Insight from Density Functional Theory, Ab Initio, and Monte Carlo Simulation Studies", Indonesian Journal of Chemistry **22** (2022) 413.

[49] K. F. Khaled & A. El-Maghraby, "Experimental, Monte Carlo and molecular dynamics simulations to investigate corrosion inhibition of mild steel in hydrochloric acid solutions", Arabian Journal of Chemistry **7** (2014) 319.

[50] S. Hadisaputra, A. A. Purwoko, A. Hakim, N. Prasetyo & S. Hamdiani, "Corrosion Inhibition Properties of Phenyl Phthalimide Derivatives against Carbon Steel in the Acidic Medium: DFT, MP2, and Monte Carlo Simulation Studies", ACS Omega **7** (2022) 33054.